The Image Foresting Transform: Recent Advances and Perspectives

Alexandre Xavier Falcão

afalcao@ic.unicamp.br

Laboratory of Visual Informatics (LIV), Institute of Computing (IC),

University of Campinas (UNICAMP)

A brief history

- This work stems from the interactive boundary delineation problem by optimum paths in an image graph (15 years ago).

A brief history

- This work stems from the interactive boundary delineation problem by optimum paths in an image graph (15 years ago).
- The most popular solution was the live-wire segmentation (show video 1).

A brief history

- This work stems from the interactive boundary delineation problem by optimum paths in an image graph (15 years ago).
- The most popular solution was the live-wire segmentation (show video 1).
- The optimum path requires the computation of an optimum-path tree rooted at its starting seed point.

A brief history

- For a set of seed points, similar algorithm provides an optimum-path forest by seed competition.

A brief history

- For a set of seed points, similar algorithm provides an optimum-path forest by seed competition.
- So, can we use this more general formulation and reduce other image problems to a local processing of the forest's attributes?

A brief history

- For a set of seed points, similar algorithm provides an optimum-path forest by seed competition.
- So, can we use this more general formulation and reduce other image problems to a local processing of the forest's attributes?
- Yes, the method is named Image Foresting Transform (IFT).

What is the IFT ?

The IFT is a tool for the design of image processing and analysis operators by choice of an adjacency relation and a connectivity function between image elements (pixels, vertices, edges, regions, or contour segments) [1].


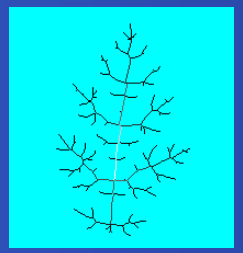
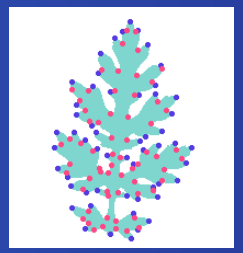
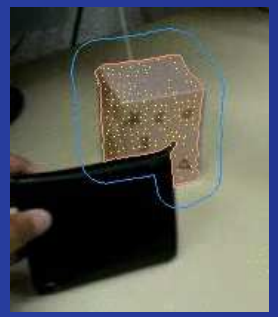
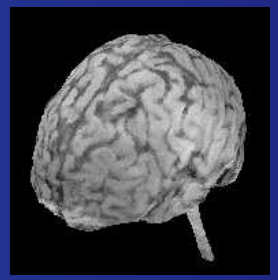
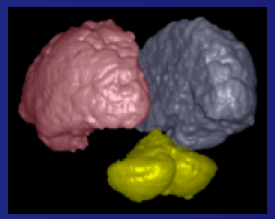

Contributors

Several colleagues and students who appear in the list of references at the end of this talk. The pdf file of the talk will be available for downloading at `www.ic.unicamp.br/~afalcao`.

Outline

- A short review on the IFT.

Outline

- A short review on the IFT.
- How to use it in image processing and analysis (a few examples).

Outline

- A short review on the IFT.
- How to use it in image processing and analysis (a few examples).
- Its recent extension to the feature space.

Outline

- A short review on the IFT.
- How to use it in image processing and analysis (a few examples).
- Its recent extension to the feature space.
- Some recent applications.

Outline

- A short review on the IFT.
- How to use it in image processing and analysis (a few examples).
- Its recent extension to the feature space.
- Some recent applications.
- Open problems, on-going works and their perspectives.

Motivation

- Unification: Several image operators are derived from a general algorithm. This favors

Motivation

- Unification: Several image operators are derived from a general algorithm. This favors
  - hardware-based implementations [2, 3],

Motivation

- Unification: Several image operators are derived from a general algorithm. This favors
  - hardware-based implementations [2, 3],
  - to understand the relation among some image operators [4, 5, 6], and

Motivation

- Unification: Several image operators are derived from a general algorithm. This favors
  - hardware-based implementations [2, 3],
  - to understand the relation among some image operators [4, 5, 6], and
  - possible extensions [7, 8, 9, 10, 11].

Motivation

- Efficiency: Most image operators can be implemented in linear time and further optimizations are possible with differential [12] and parallel [13] computation, and for some specific applications [14, 15].

Motivation

- Efficiency: Most image operators can be implemented in linear time and further optimizations are possible with differential [12] and parallel [13] computation, and for some specific applications [14, 15].
- Simplicity: The image operators are reduced to the choice of two parameters in the IFT algorithm and a local processing of its output.

What kind of problems can be solved?

Problems which are either directly or indirectly related to an optimal image (set) partition.

- Distance transforms and related operators: Multiscale skeletonization [16], fractal dimensions [17], shape filtering [14, 16], shape description by saliences and tensor scale [17, 18, 19, 20], geodesic paths [1].

What kind of problems can be solved?

- Filtering and Segmentation:
  Morphological reconstructions [4] and image segmentation based on watershed transforms [5, 12, 7, 21], pixel clustering [10], contour tracking [22, 15, 23], tree pruning [9, 24], graph-cut measures [8], and fuzzy-connected components [25, 26].
- Pattern recognition:
  Fast supervised and unsupervised learning approaches [10, 11, 27, 28].

Images as graphs

The image is interpreted as a graph whose nodes are the pixels and the arcs are defined by an adjacency relation $\mathcal{A}$: $(s,t) \in \mathcal{A}$ if $\|t-s\| \leq d_i$.

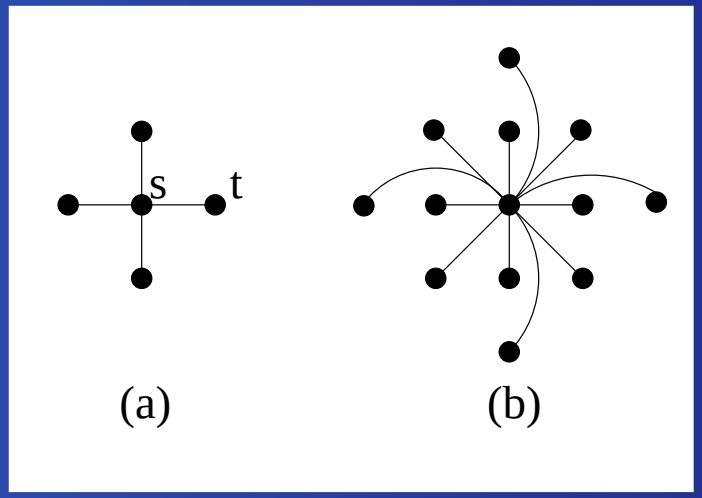

(a) $d_i = 1$ and (b) $d_i = 2$.

Paths in the graph

- A path π_t is a sequence of adjacent nodes with terminus at some node t and $\pi_t = \langle t \rangle$ is said trivial.

Paths in the graph

- A path π_t is a sequence of adjacent nodes with terminus at some node t and $\pi_t = \langle t \rangle$ is said trivial.
- The predecessor $P(s)$ of each node $s \in \pi_t$ leads to a root node $R(t)$ and $P(R(t)) = nil$.

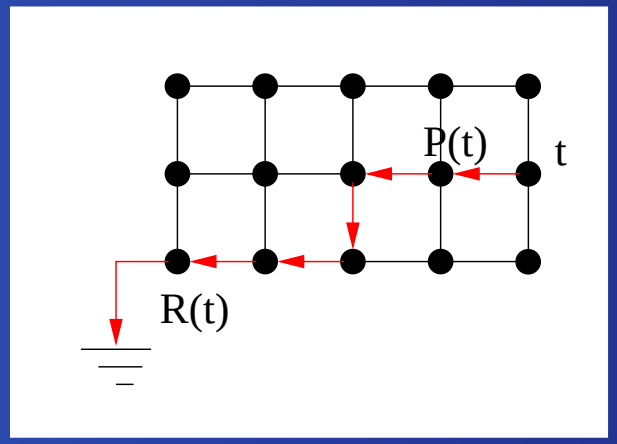

Optimum paths

- A connectivity function $f(\pi_t)$ assigns a value to any path π_t.

Optimum paths

- A connectivity function $f(\pi_t)$ assigns a value to any path π_t.
- A path π_t is optimum if $f(\pi_t) \leq f(\tau_t)$ for any other τ_t, irrespective to its root.

Optimum paths

- A connectivity function $f(\pi_t)$ assigns a value to any path π_t.
- A path π_t is optimum if $f(\pi_t) \leq f(\tau_t)$ for any other τ_t, irrespective to its root.
- The dual definition $f(\pi_t) \geq f(\tau_t)$ is also valid.

The IFT

- From an initial path-value map $V_0(t) = f(\langle t \rangle)$ where all nodes are trivial paths.

The IFT

- From an initial path-value map $V_0(t) = f(\langle t \rangle)$ where all nodes are trivial paths.
- The IFT computes a minimal (maximal) path-value map $V(t) = \min_{\forall \pi_t}\{f(\pi_t)\}$ for every node t.

The IFT

- From an initial path-value map $V_0(t) = f(\langle t \rangle)$ where all nodes are trivial paths.
- The IFT computes a minimal (maximal) path-value map $V(t) = \min_{\forall \pi_t}\{f(\pi_t)\}$ for every node t.
- The result is an optimum-path forest P — an acyclic graph where all paths are optimum according to f.

The IFT computation

- The first roots are identified as the global minima (maxima) of V_0.

The IFT computation

- The first roots are identified as the global minima (maxima) of V_0.
- They may conquer their adjacent nodes by offering them better paths.

The IFT computation

- The first roots are identified as the global minima (maxima) of V_0.
- They may conquer their adjacent nodes by offering them better paths.
- The process continues from the adjacent nodes in a non-decreasing (non-increasing) order of path value.

$$\text{if } f(\pi_s \cdot \langle s,t \rangle) < f(\pi_t) \quad \text{then } \pi_t \leftarrow \pi_s \cdot \langle s,t \rangle.$$

Segmentation by seed competition(IFTSC)

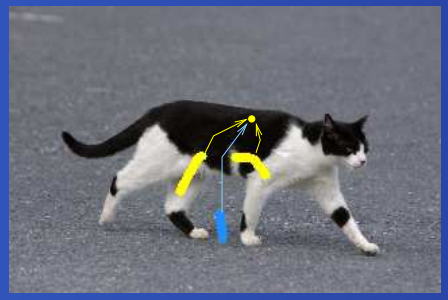

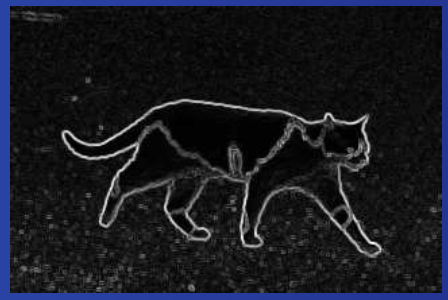

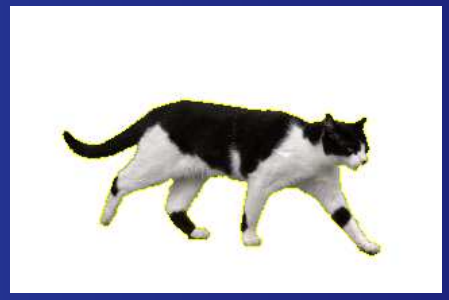

Segmentation by seed competition(IFTSC)

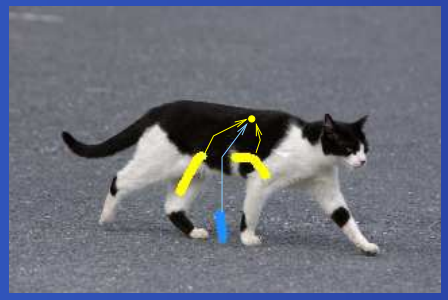

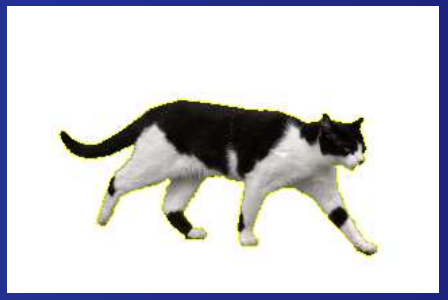

- An optimum-path forest is computed by assigning each pixel to its most strongly connected marker pixel.

Segmentation by seed competition(IFTSC)

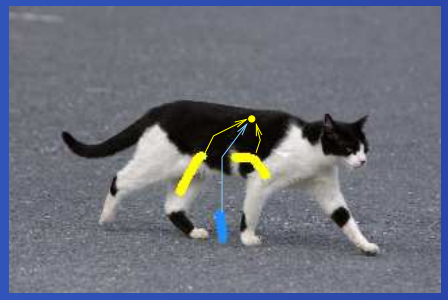

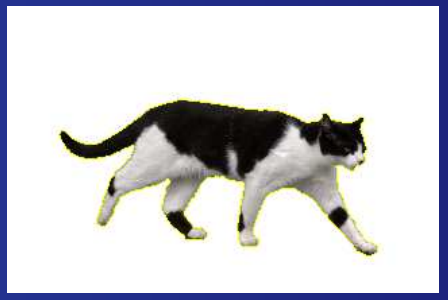

- An optimum-path forest is computed by assigning each pixel to its most strongly connected marker pixel.
- The object is defined by the union of optimum-path trees rooted in the object markers (show videos 2 and 3).

Segmentation by seed competition(IFTSC)

An image-graph where arc weights $w(s,t)$ indicate the dissimilarity between adjacent nodes and we wish to compute V such that the roots of P belong to a seed set $\mathcal{S} = \{(3,3),(5,1)\}$.

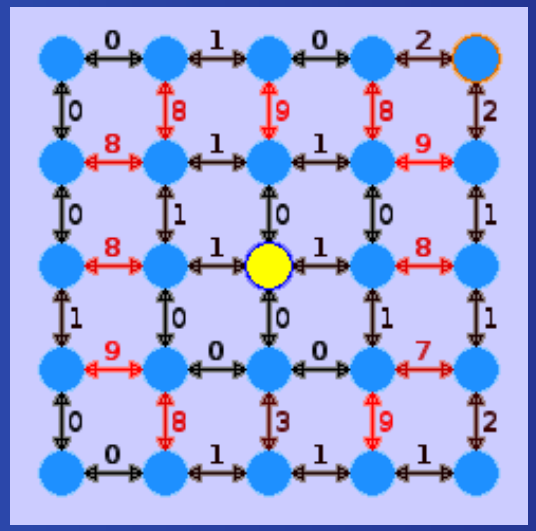

its path function

We need to define a path-initialization rule and a path-extension rule. The path-value map V is minimized for function f_1.

$$f_1(\langle t \rangle) = \begin{cases} 0 & \text{if } t \in \mathcal{S} \\ +\infty & \text{otherwise} \end{cases}$$

$$f_1(\pi_s \cdot \langle s, t \rangle) = \max\{f_1(\pi_s), w(s,t)\}$$

Path propagation

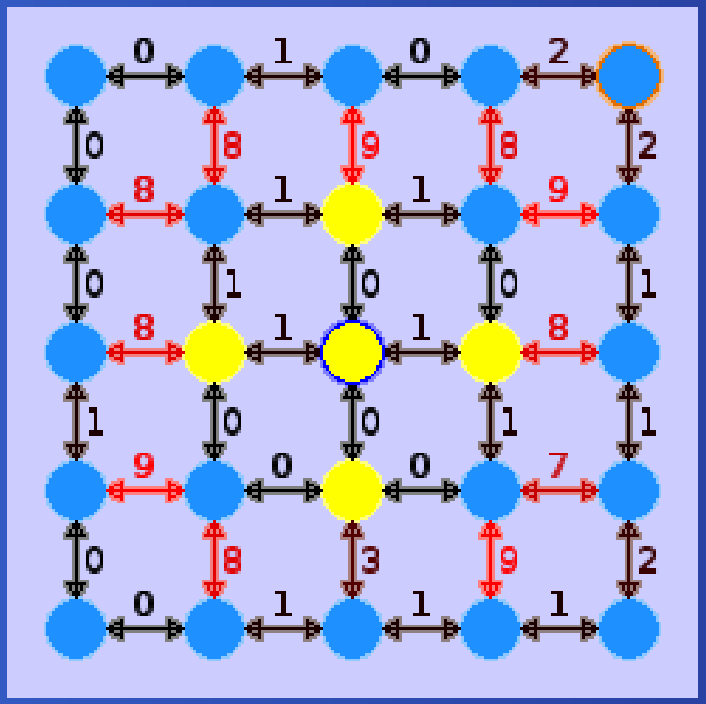

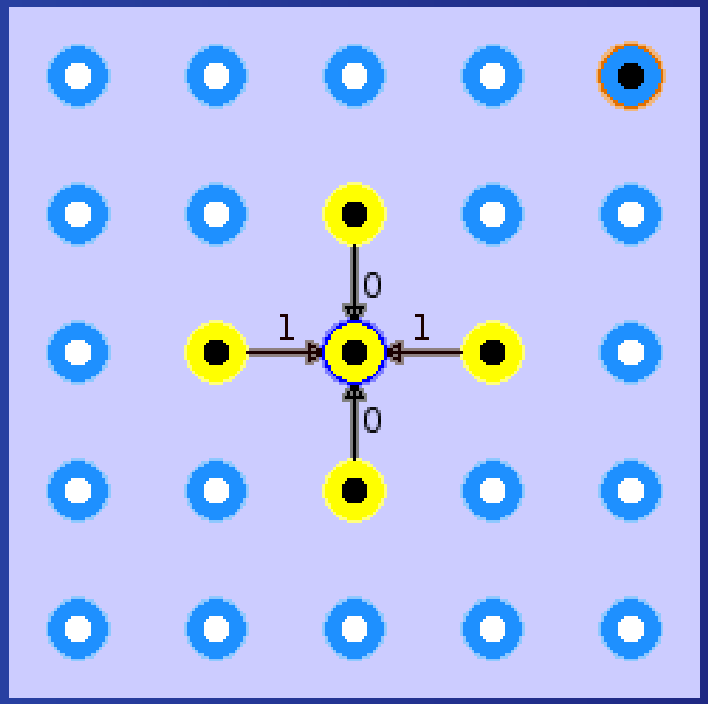

Path propagation

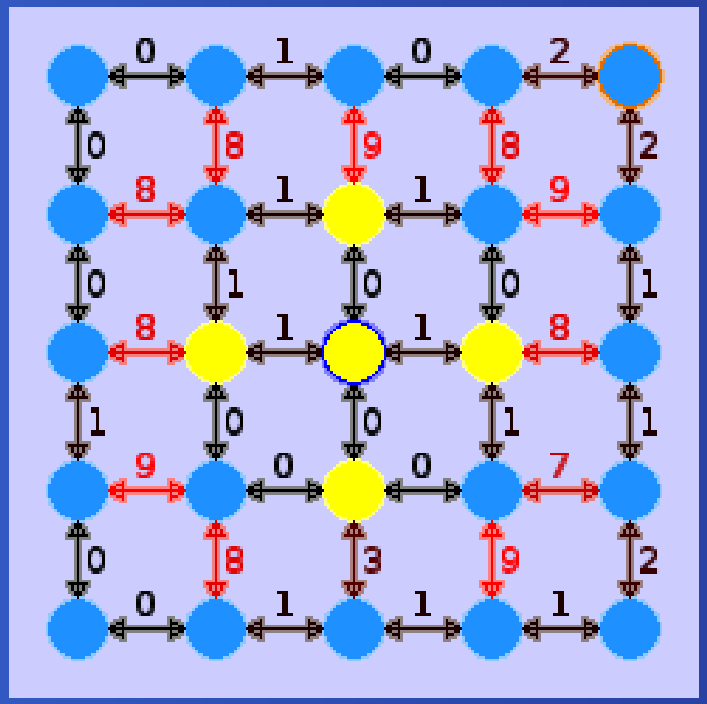

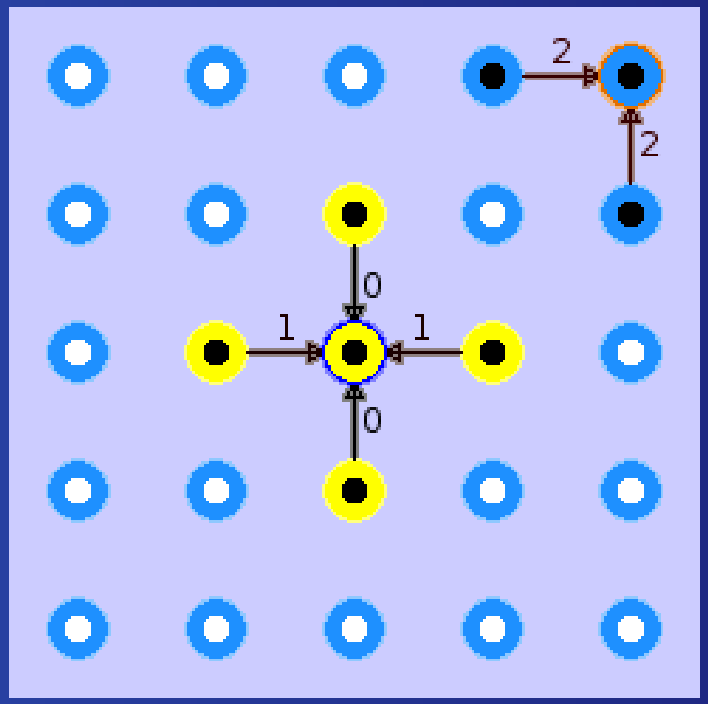

Path propagation

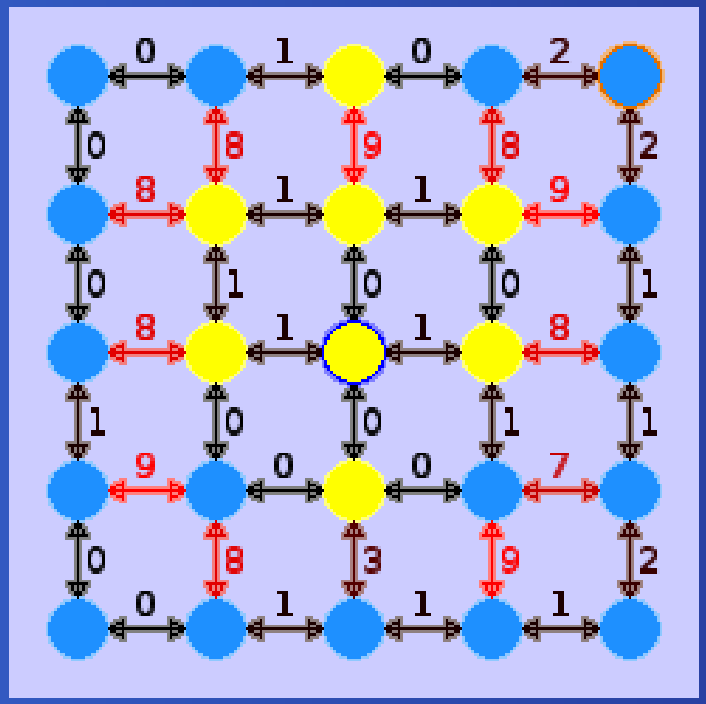

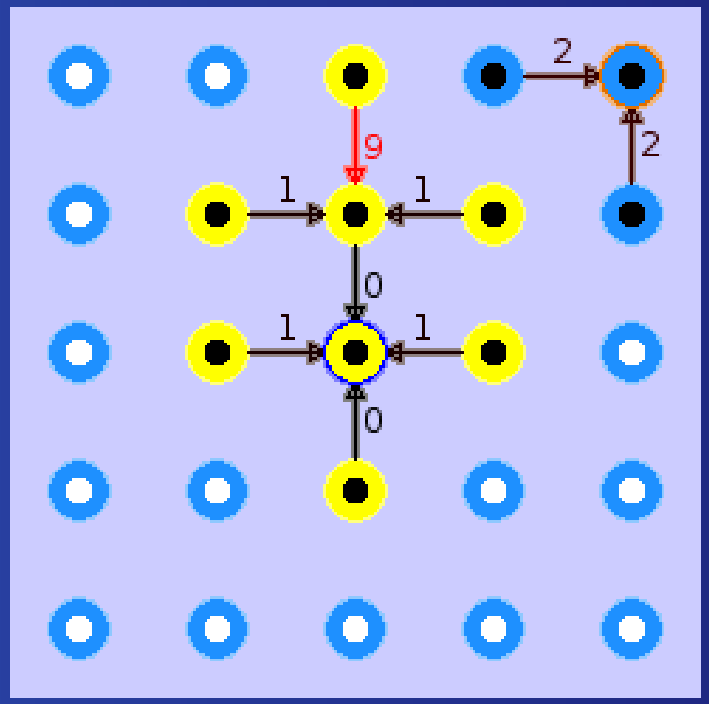

Path propagation

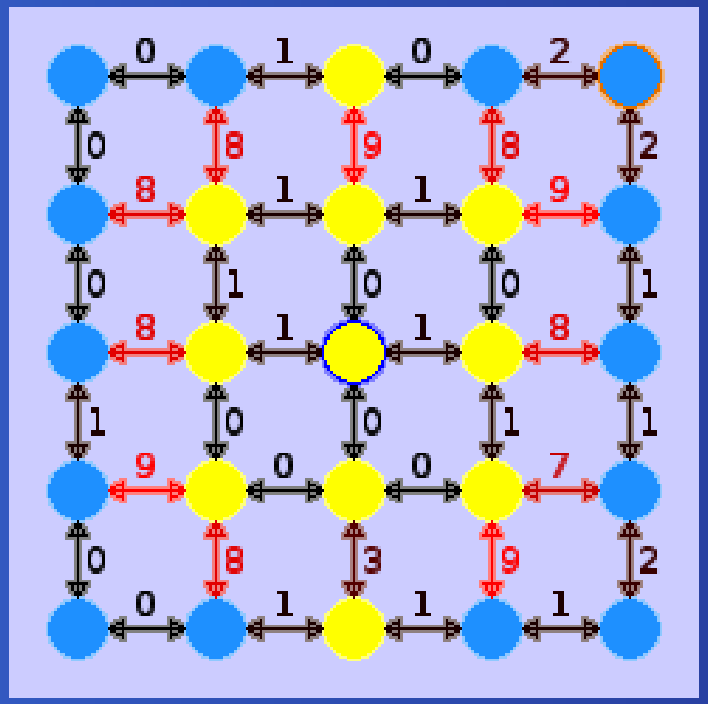

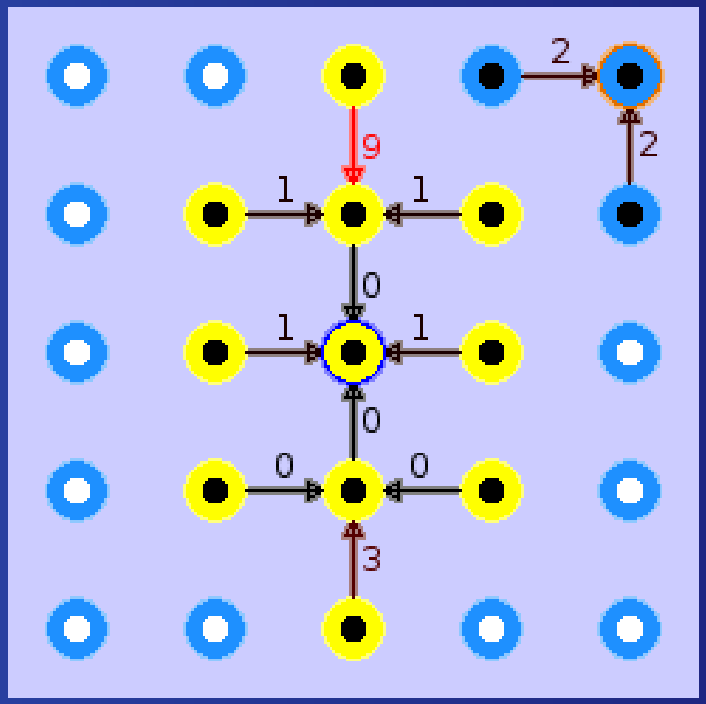

Path propagation

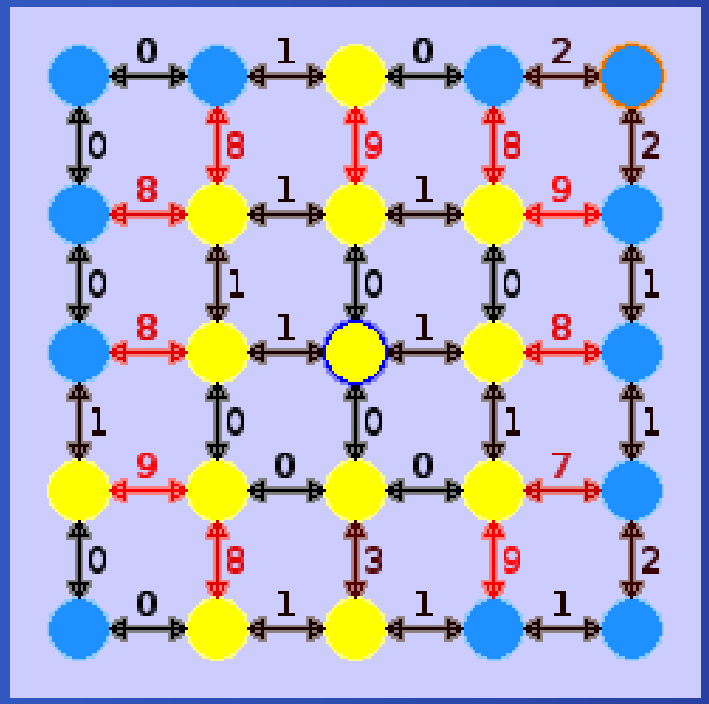

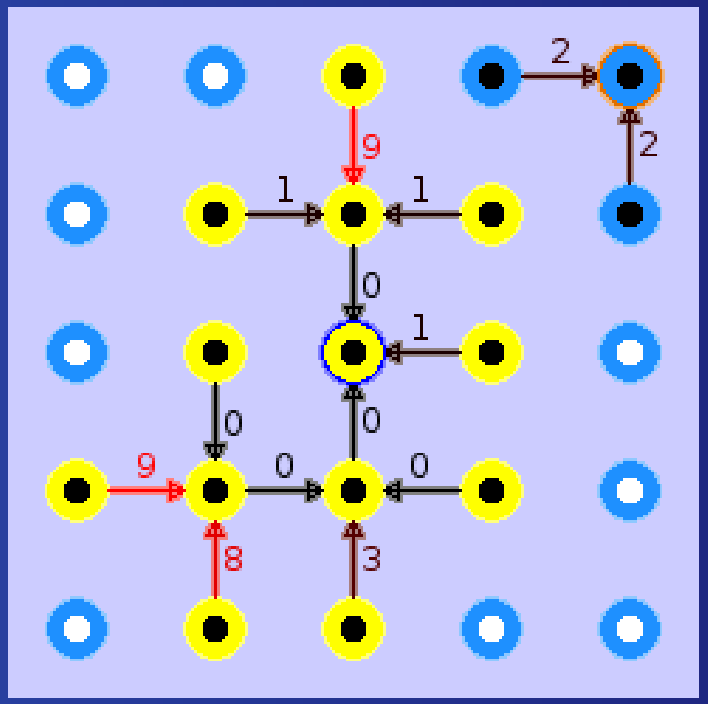

Path propagation

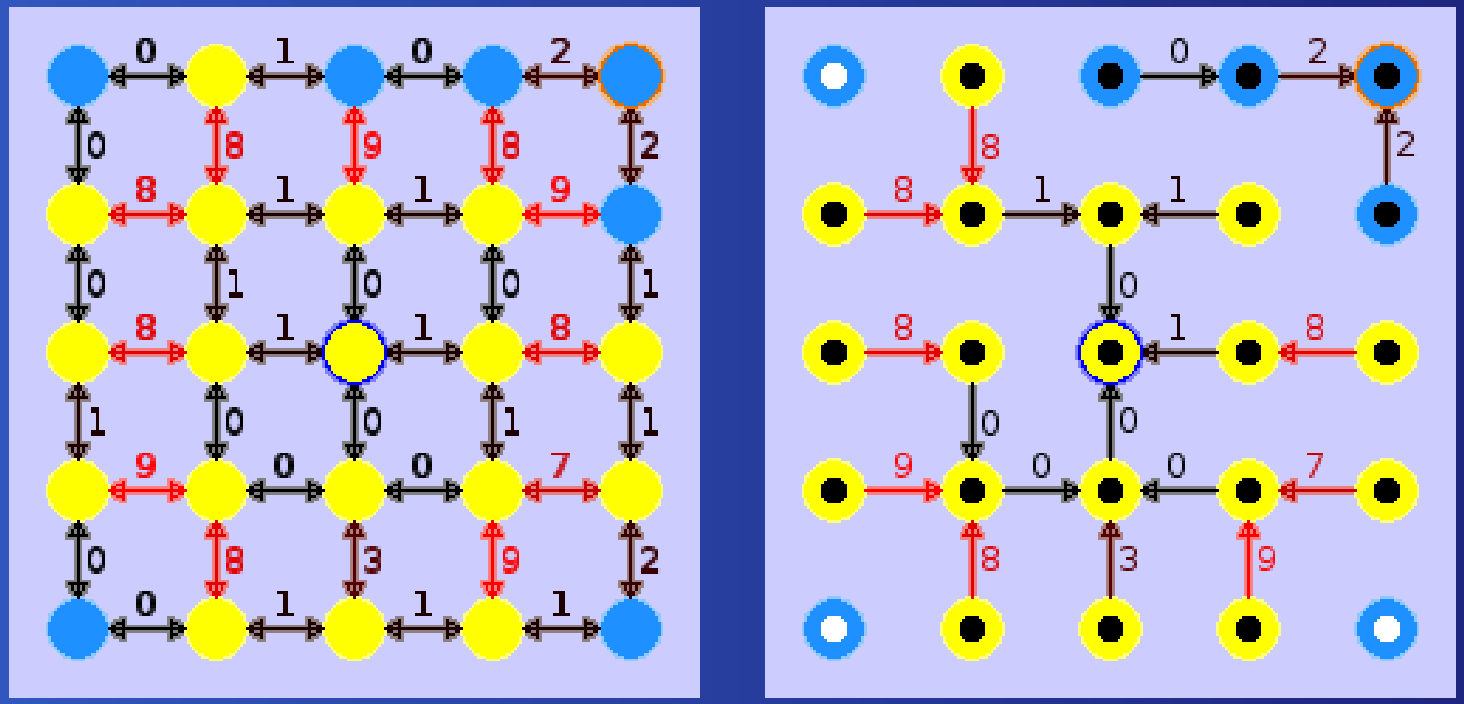

after 12 iterations.

Path propagation

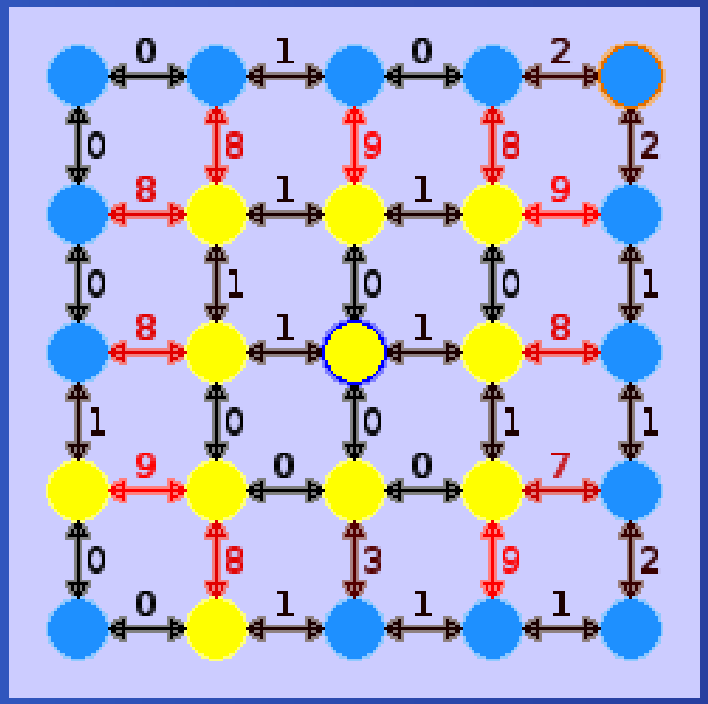

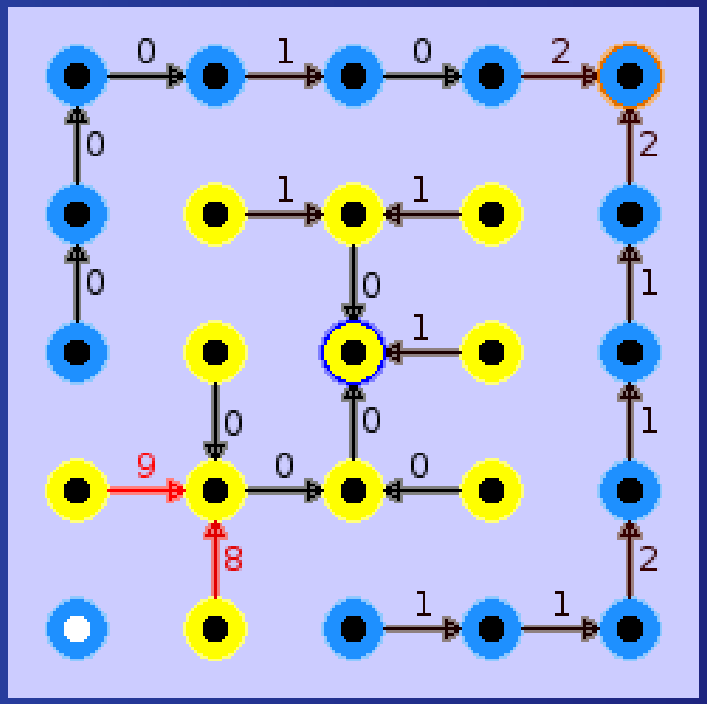

after 20 iterations.

Path propagation

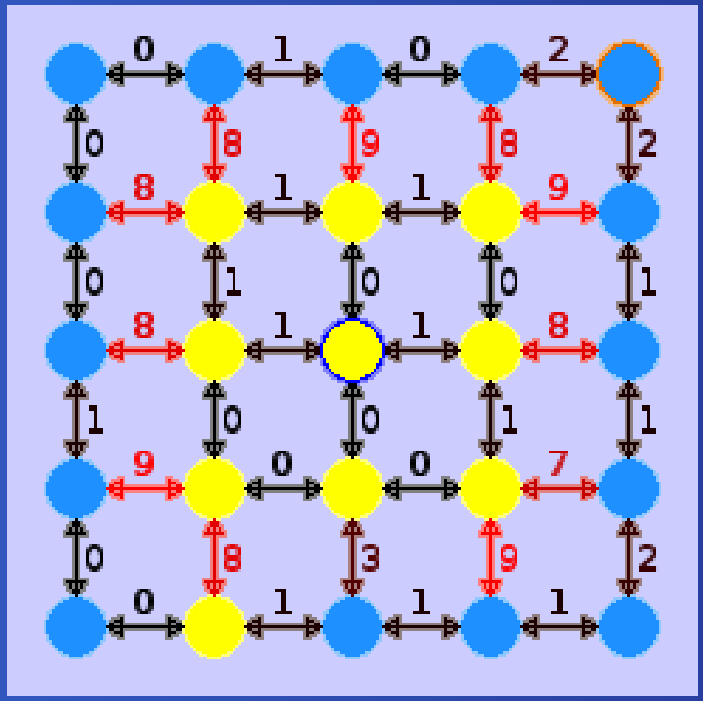

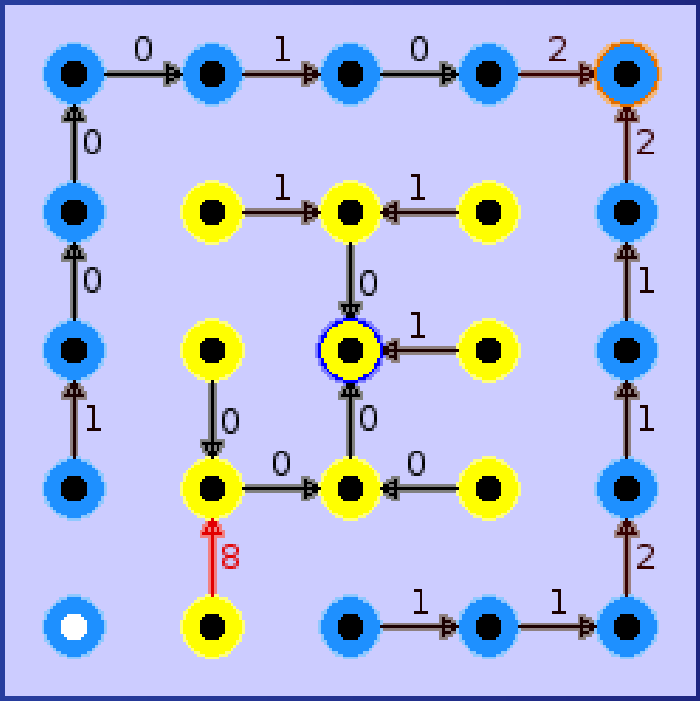

Path propagation

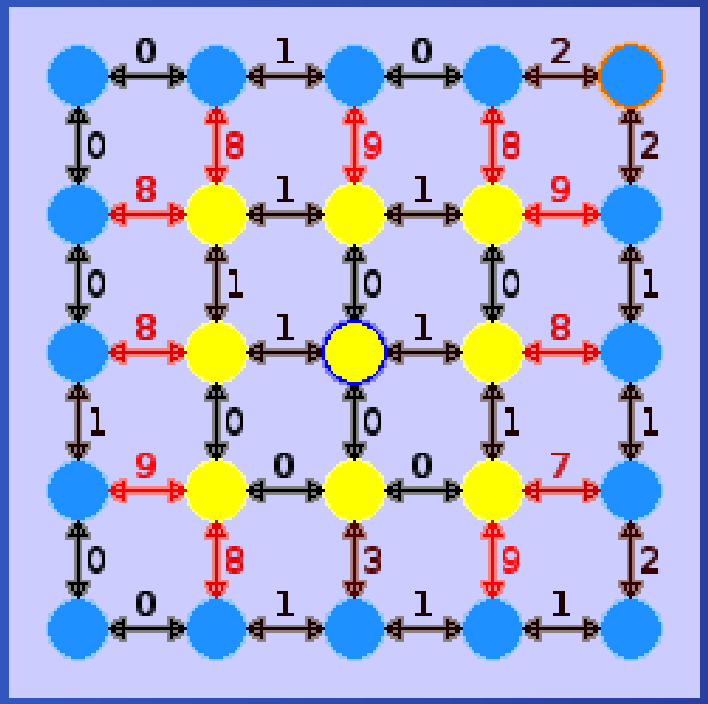

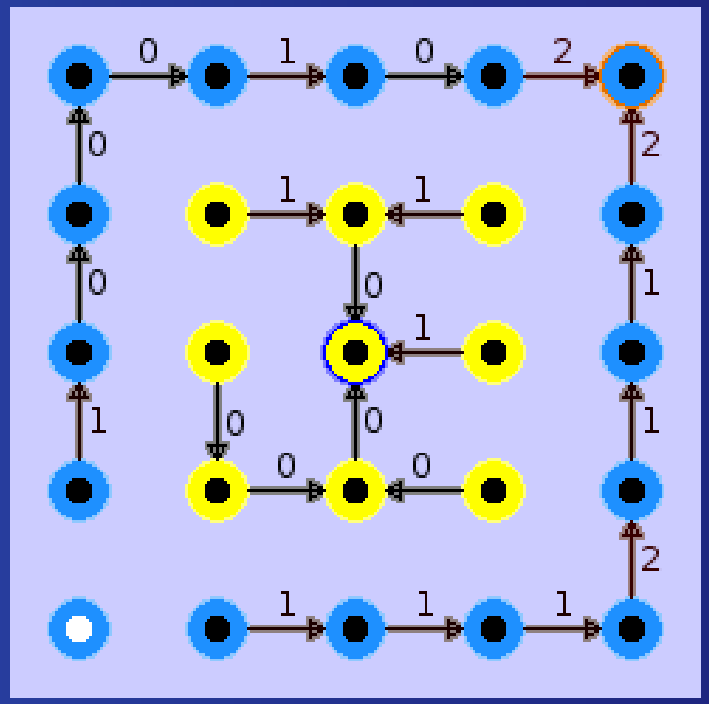

Path propagation

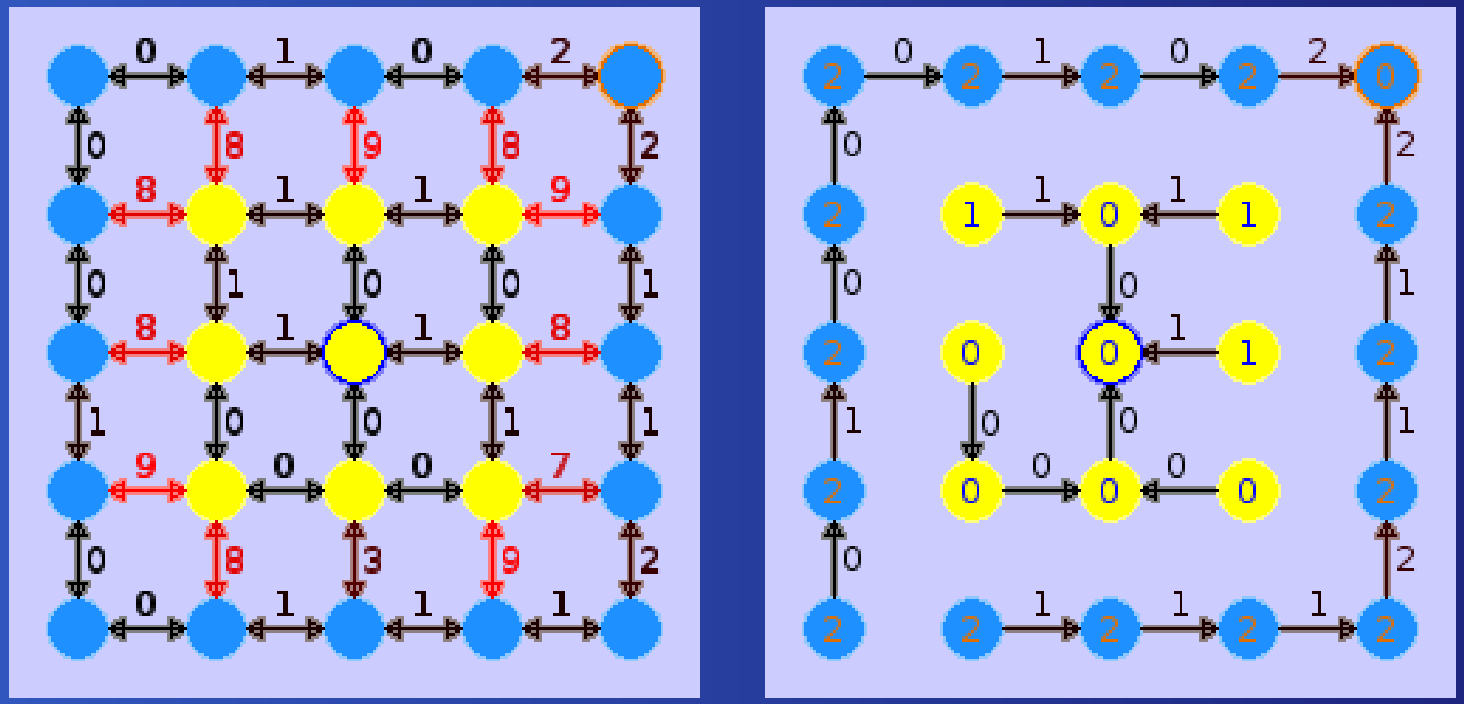

after 25 iterations.

Information propagation

- The IFT requires a priority queue Q for path propagation (modified Dijkstra's algorithm).

Information propagation

- The IFT requires a priority queue Q for path propagation (modified Dijkstra's algorithm).
- A root s is an optimum trivial path $\langle s \rangle$, such that $P(s) = nil$ when s is removed from Q.

Information propagation

- The IFT requires a priority queue Q for path propagation (modified Dijkstra's algorithm).
- A root s is an optimum trivial path $\langle s \rangle$, such that $P(s) = nil$ when s is removed from Q.
- It can propagate other informations to each node: a root label [12, 21], its propagation order [26], a graph-cut measure [8], etc.

Information propagation

- The IFT requires a priority queue Q for path propagation (modified Dijkstra's algorithm).
- A root s is an optimum trivial path $\langle s \rangle$, such that $P(s) = nil$ when s is removed from Q.
- It can propagate other informations to each node: a root label [12, 21], its propagation order [26], a graph-cut measure [8], etc.
- The operators result from a local processing of one or more of these informations.

its correctness

For every node t, there must exist at least one optimum path π_t which is either trivial or has the form $\pi_s \cdot \langle s, t \rangle$ where:

1. $f(\pi_s) \leq f(\pi_t)$.
2. π_s is optimum.
3. For any optimum path τ_s, $f(\tau_s \cdot \langle s, t \rangle) = f(\pi_t)$.

These conditions are applied to only optimum paths.

Euclidean distance transform (EDT)

The EDT of a pixel set $\mathcal{S}$ uses Euclidean adjacency $\mathcal{A}$ and minimizes V for f_2 [16].

$$f_2(\langle t \rangle) = \begin{cases} 0 & \text{if } t \in \mathcal{S} \\ +\infty & \text{otherwise} \end{cases}$$

$$f_2(\pi_s \cdot \langle s, t \rangle) = \|t - R(s)\|$$

where $R(s)$ is the root of s.

EDT with Label Propagation

A consecutive integer number can be assigned to each contour pixel in $\mathcal{S}$ and propagated to the rest of the image.

Multiscale skeletons

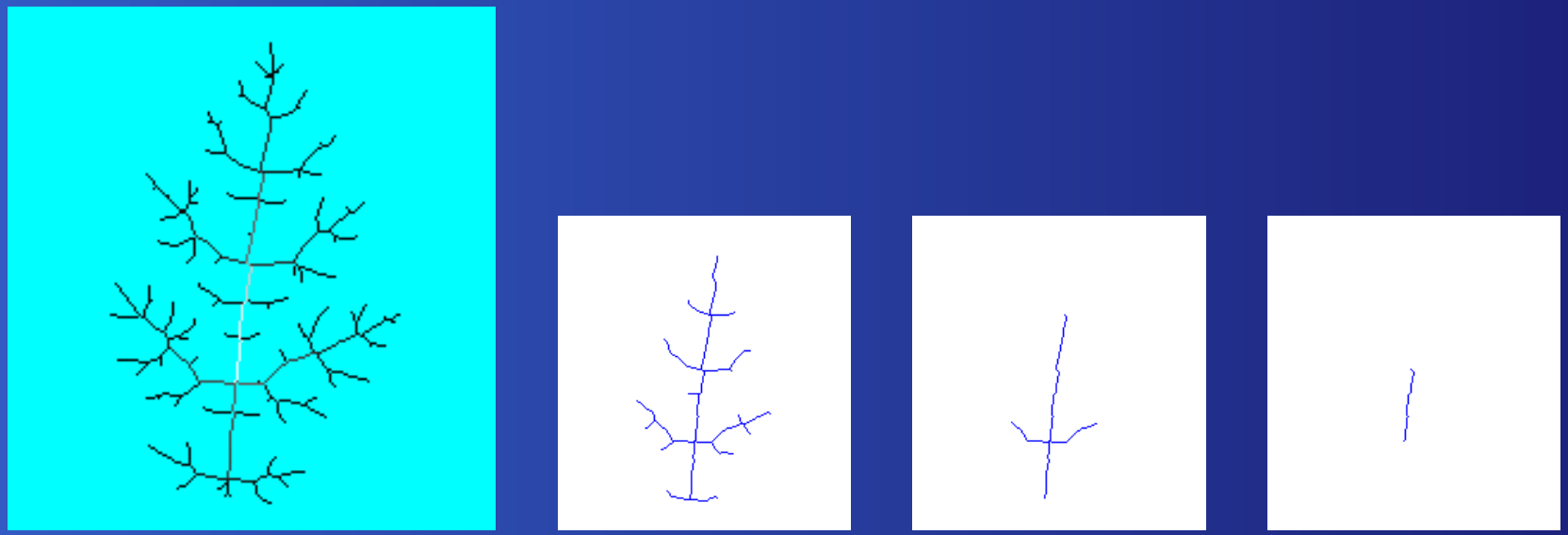

A difference image is obtained from the labeled image. Increasing thresholds create more simplified one-pixel-wide and connected skeletons.

Skeletons of multiples contours

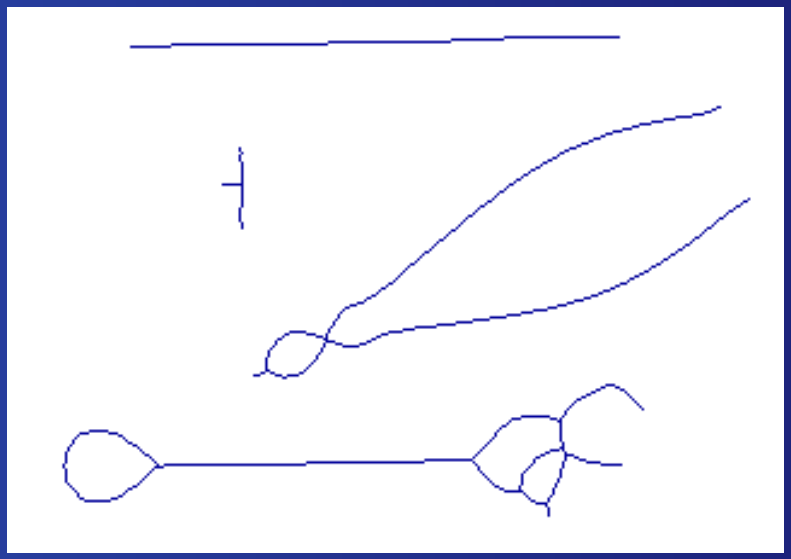

The method is easily extended to incorporate the SKIZ in the case of multiple contours.

Shape saliences

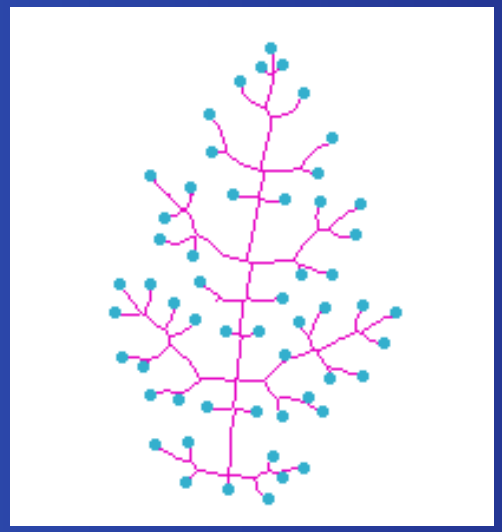

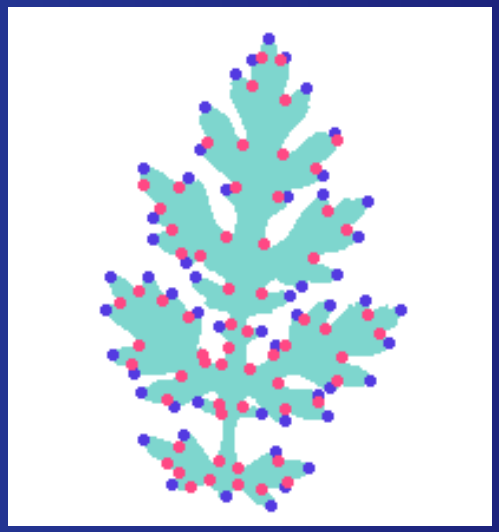

Skeleton saliences are detected from the aperture angles of their influence zones within a small dilation radius, leading to contour saliences [17].

Live-wire-on-the-fly (IEEE TMI, 2000)

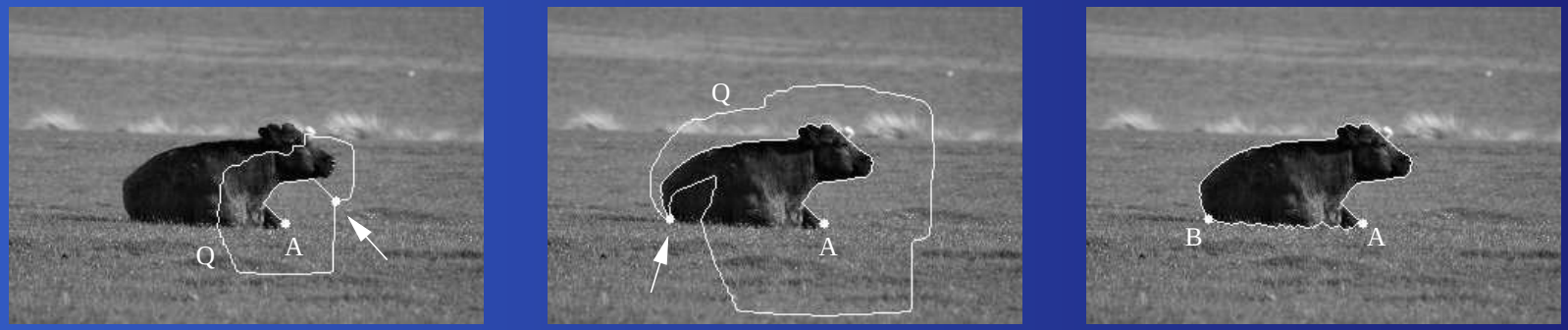

Live-wire-on-the-fly solves the boundary delineation problem with real time response to the user's actions, independently of the image size [15].

its path function

The minimization of V for path function f_3 allows longer and oriented segments.

$$f_3(\langle t \rangle) = \begin{cases} 0 & \text{if } t \in \mathcal{S} \\ +\infty & \text{otherwise} \end{cases}$$

$$f_3(\pi_s \cdot \langle s,t \rangle) = \begin{cases} f_3(\pi_s) + w^a(s,t) & \text{if } L(s,t) < R(s,t) \\ f_3(\pi_s) + K & \text{otherwise} \end{cases}$$

for $0 \leq w^a(s,t) \leq K$, $a > 0$, $L(s,t)$ and $R(s,t)$ are intensities on the left and right sides of arc (s,t).

Multiple object segmentation

Multiple objects are segmented by using a gradient image I and initial path values $V_0(t) = H(t) > I(t)$ [4, 7].

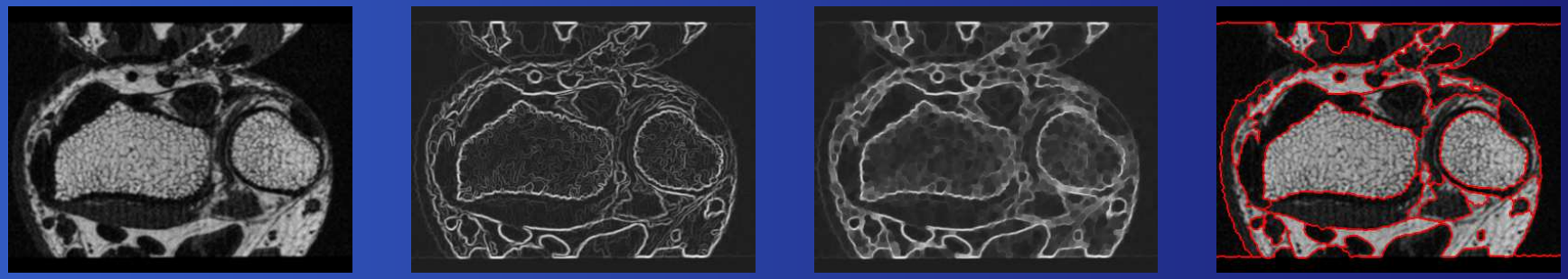

H is the closing of I plus 1, using adjacency radius $d_i = 2.5$. The IFT uses adjacency radius $d_i = 3.5$ and path function f_4 for segmentation.

its path function

A label map L is obtained by minimizing V for f_4.

$$f_4(\langle t \rangle) = \begin{cases} I(t) & \text{if } t \in \mathcal{R} \\ H(t) & \text{otherwise} \end{cases}$$

$$f_4(\pi_s \cdot \langle s, t \rangle) = \max\{f_4(\pi_s), I(t)\}$$

where $\mathcal{R}$ is the root set whose pixels come from some minima of H. Initially, $f_4(\langle t \rangle) = H(t)$ for all t, then the roots are identified on-the-fly: if $P(t) = nil$ when t is removed from Q then $t \in \mathcal{R}$ and $f_4(\langle t \rangle) \leftarrow I(t)$ for label propagation.

Extension to the feature space

- The graph nodes may be images, shapes, regions or other entities of a dataset.

Extension to the feature space

- The graph nodes may be images, shapes, regions or other entities of a dataset.
- Each node s is represented by a feature vector $\vec{v}(s)$ of n dimensions.

Extension to the feature space

- The graph nodes may be images, shapes, regions or other entities of a dataset.
- Each node s is represented by a feature vector $\vec{v}(s)$ of n dimensions.
- The similarity between adjacent nodes is given by a distance function $d(s,t)$ (e.g., $d(s,t) = \|\vec{v}(t) - \vec{v}(s)\|$).

Extension to the feature space

- The graph nodes may be images, shapes, regions or other entities of a dataset.
- Each node s is represented by a feature vector $\vec{v}(s)$ of n dimensions.
- The similarity between adjacent nodes is given by a distance function $d(s,t)$ (e.g., $d(s,t) = \|\vec{v}(t) - \vec{v}(s)\|$).
- The graph is usually weighted on the arcs by $d(s,t)$ and may also be weighted on the nodes by a probability density function $\rho(s)$.

How do we create arcs in this case?

The adjacency relation may be complete, may consider maximum distances around the nodes or may take into account the k-nearest nodes (k-nn graph). For example:

$\mathcal{A}_k$: $(s,t) \in \mathcal{A}_k$ (or $t \in \mathcal{A}_k(s)$) if t is k nearest neighbor of s in the feature space.

The best value of k can be computed by several different ways, depending on the learning approach: supervised or unsupervised.

Clustering by OPF

The graph is weighted on the arcs $(s,t) \in \mathcal{A}_k$ by $d(s,t)$ and on the nodes by the pdf $\rho(s)$ [10].

$$\rho(s) = \frac{1}{\sqrt{2\pi\sigma^2}|\mathcal{A}_k(s)|} \sum_{\forall t \in \mathcal{A}_k(s)} \exp\left(\frac{-d^2(s,t)}{2\sigma^2}\right)$$

where $\sigma = \frac{d_f}{3}$ and $d_f = \max_{\forall (s,t) \in \mathcal{A}_k}\{d(s,t)\}$. The best value of k is found as the one whose clustering produces a minimum normalized cut in the k-nn graph.

its path function

We maximize V for path function f_5.

$$f_5(\langle t \rangle) = \begin{cases} \rho(t) & \text{if } t \in \mathcal{R} \\ H(t) & \text{otherwise} \end{cases}$$

$$f_5(\pi_s \cdot \langle s, t \rangle) = \min\{f_5(\pi_s), \rho(t)\}$$

where $\rho(t) > H(t)$, $H(t)$ can be the result of some anti-extensive operation on ρ, and $\mathcal{R}$ is the root set found on-the-fly ($P(t) = nil$ when t is removed from Q).

Example

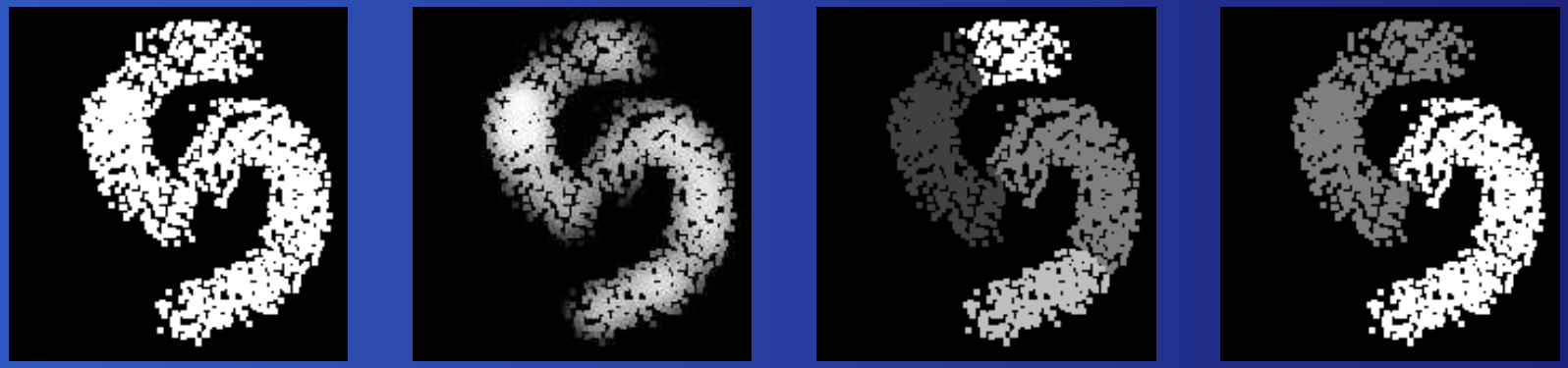

(a) (b) (c) (d)

Each cluster in (c) is an optimum-path tree rooted at one maximum of the pdf shown in (b). Irrelevant clusters can be eliminated by choice of H, as shown in (d). The method is shape independent.

Some recent applications

- A graph-based framework for fast interactive segmentation of natural images [29].

Some recent applications

- A graph-based framework for fast interactive segmentation of natural images [29].
- Texture image recognition [30].

Some recent applications

- A graph-based framework for fast interactive segmentation of natural images [29].
- Texture image recognition [30].
- Spoken emotion recognition [31].

Some recent applications

- A graph-based framework for fast interactive segmentation of natural images [29].
- Texture image recognition [30].
- Spoken emotion recognition [31].
- Fingerprint and face recognition [32, 33, 34].

Some recent applications

- A graph-based framework for fast interactive segmentation of natural images [29].
- Texture image recognition [30].
- Spoken emotion recognition [31].
- Fingerprint and face recognition [32, 33, 34].
- Remote sensing: land use classification [35] and rainfall estimation [36].

Some recent applications

- Object tracking in video [37].

Some recent applications

- Object tracking in video [37].
- Cloud bank model for automatic structure segmentation [38, 39].

Some recent applications

- Object tracking in video [37].
- Cloud bank model for automatic structure segmentation [38, 39].
- Automatic brain tissue classification in MR images [40, 10] using clustering by OPF.

Some recent applications

- Object tracking in video [37].
- Cloud bank model for automatic structure segmentation [38, 39].
- Automatic brain tissue classification in MR images [40, 10] using clustering by OPF.
- Oropharyngeal dysphagia identification and laryngeal pathology detection [41, 42].

Object tracking in video

1. Starting from the interactive segmentation by IFTSC in a first frame.

Object tracking in video

1. Starting from the interactive segmentation by IFTSC in a first frame.
2. Motion estimation is constrained within the object mask.

Object tracking in video

1. Starting from the interactive segmentation by IFTSC in a first frame.
2. Motion estimation is constrained within the object mask.
3. The average motion is applied to an external marker around the object.

Object tracking in video

1. Starting from the interactive segmentation by IFTSC in a first frame.
2. Motion estimation is constrained within the object mask.
3. The average motion is applied to an external marker around the object.
4. New internal and external markers are selected for automatic segmentation by IFTSC in the next frame, and the process is repeated from 2 (show video 4).

Cloud bank segmentation

- The method is divided in two steps: training and execution.

Cloud bank segmentation

- The method is divided in two steps: training and execution.
- In training, a discrete shape model is created to guide the delineation process.

Cloud bank segmentation

- The method is divided in two steps: training and execution.
- In training, a discrete shape model is created to guide the delineation process.
- In execution, delineation by IFT provides a candidate object for each position of the shape model on the image and a criterion function assigns a score to that candidate.

Cloud bank segmentation

- The method is divided in two steps: training and execution.
- In training, a discrete shape model is created to guide the delineation process.
- In execution, delineation by IFT provides a candidate object for each position of the shape model on the image and a criterion function assigns a score to that candidate.
- Segmentation is defined by the object with the highest score.

Cloud bank training

- A set of training objects is provided to capture the shape variations of a given structure.

Cloud bank training

- A set of training objects is provided to capture the shape variations of a given structure.
- The objects are translated to a common reference point and their 0/1 values are averaged.

Cloud bank training

- A set of training objects is provided to capture the shape variations of a given structure.
- The objects are translated to a common reference point and their 0/1 values are averaged.
- The idea is to avoid registration in training and execution.

Cloud bank training

The training creates a cloud image, with an uncertainty region, which should include the object's boundary for some image location.

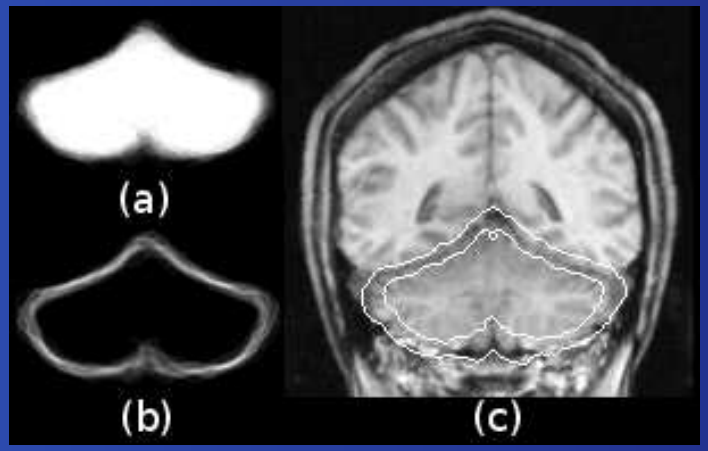

Cloud bank training

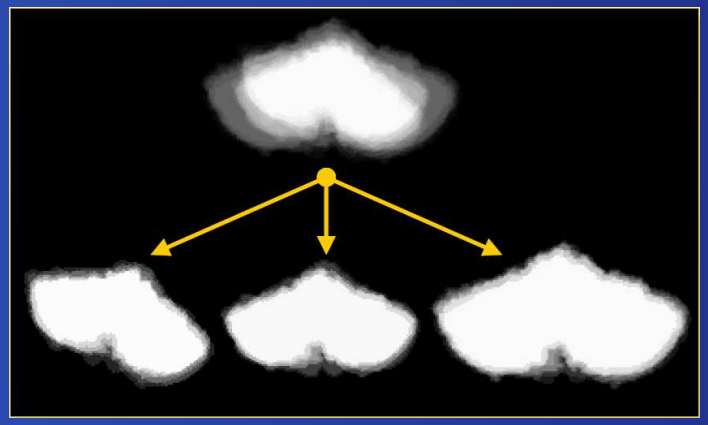

To encode shape variations with narrower uncertainty regions, the objects are grouped by maximal cliques on a complete graph weighted by their similarity values, forming a cloud bank.

Cloud execution: brain segmentation

- For brain segmentation, the image is first aligned by the mid-sagital plane (MSP) and the search is performed in multiple scales.

Cloud execution: brain segmentation

- For brain segmentation, the image is first aligned by the mid-sagital plane (MSP) and the search is performed in multiple scales.
- Each cloud moves over the MSP and, for each position, delineation is done by IFTSC inside the uncertainty region.

Cloud execution: brain segmentation

- For brain segmentation, the image is first aligned by the mid-sagital plane (MSP) and the search is performed in multiple scales.
- Each cloud moves over the MSP and, for each position, delineation is done by IFTSC inside the uncertainty region.
- The mean graph cut is used to assign scores to the candidate objects.

Cloud execution: brain segmentation

- For brain segmentation, the image is first aligned by the mid-sagital plane (MSP) and the search is performed in multiple scales.
- Each cloud moves over the MSP and, for each position, delineation is done by IFTSC inside the uncertainty region.
- The mean graph cut is used to assign scores to the candidate objects.
- Execution takes about 1 min for 4 clouds in a modern PC.

2D example in brain segmentation

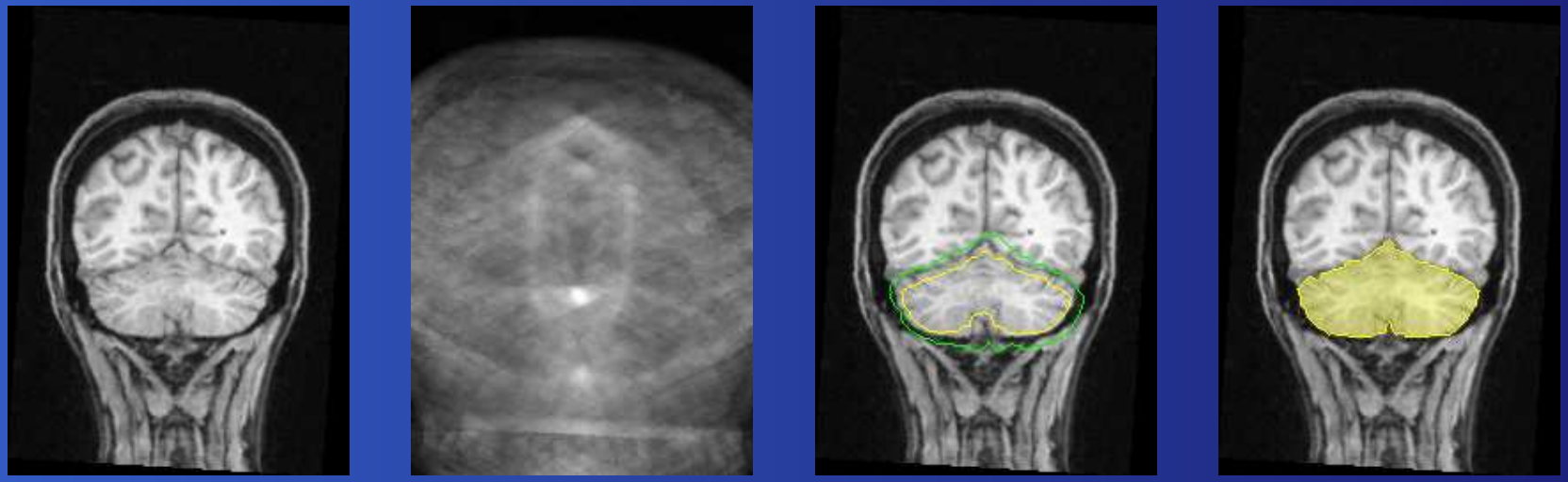

(a) Input image. (b) The recognition score for all positions. (c) The best location. (d) Final segmentation.

3D results in brain segmentation

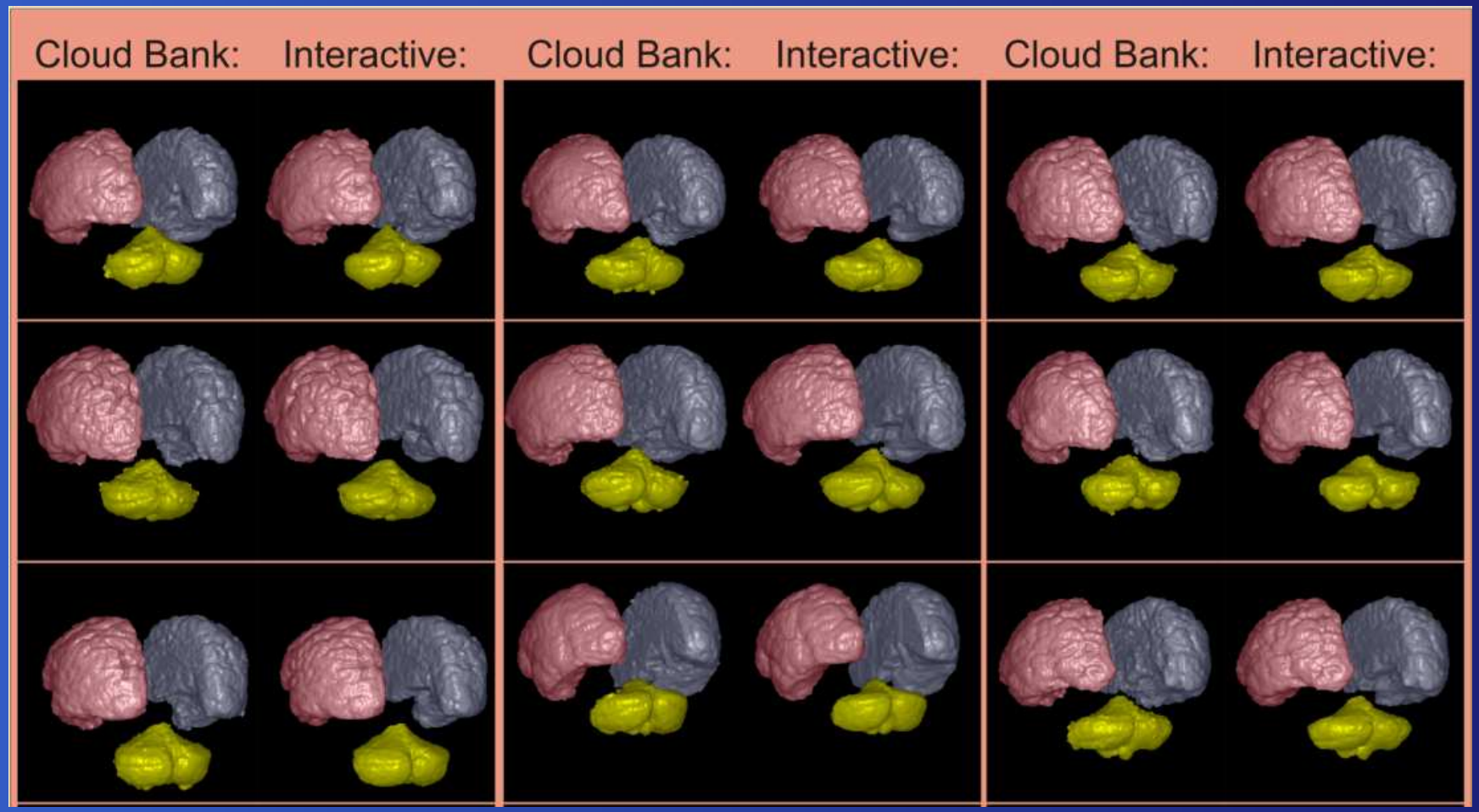

3D results in brain segmentation

Evaluation on a dataset with 40 MR images of normal subjects from both genders and ages from 9 to 49 years (Dice similarities).

Object	Mean	S.dev
brain (GM+WM)	97.37	0.46
hemispheres	97.59	0.48
cerebellum	94.97	0.84
right hemisphere	97.16	0.48
left hemisphere	97.05	0.55

Some open problems

- Parallel IFT in multi-core platforms.

Some open problems

- Parallel IFT in multi-core platforms.
- Cloud-based image segmentation for different applications and using other IFT-based operators for delineation.

Some open problems

- Parallel IFT in multi-core platforms.
- Cloud-based image segmentation for different applications and using other IFT-based operators for delineation.
- OPF-based learning algorithms for large datasets and their applications in segmentation, content-based image retrieval, super-resolution and image compression problems.

On-going works and their perspectives

- An IFT-based hardware architecture for image processing.

On-going works and their perspectives

- An IFT-based hardware architecture for image processing.
- IFT-based tracking of multiple objects with occlusion.

On-going works and their perspectives

- An IFT-based hardware architecture for image processing.
- IFT-based tracking of multiple objects with occlusion.
- MR-image segmentation of brain structures by cloud bank.

On-going works and their perspectives

- An IFT-based hardware architecture for image processing.
- IFT-based tracking of multiple objects with occlusion.
- MR-image segmentation of brain structures by cloud bank.
- Brain tissue classification of segmented structures by OPF clustering.

Acknowledgments

Thank you!!!

UNICAMP, FAPESP and CNPq.

References

[1] A.X. Falcão, J. Stolfi, and R.A. Lotufo. The image foresting transform: Theory, algorithms, and applications. *IEEE Trans. on Pattern Analysis and Machine Intelligence*, 26(1):19–29, 2004.

[2] F. Cappabianco, G. Araújo, and A.X. Falcão. The image foresting transform architecture. In *IEEE Intl. Conf. on Field Programmable Technology (ICFPT)*, pages 137–144, Kokurakita, Kitakyushu, Japan, Dec 2007.

[3] F. Cappabianco, G. Araujo, R. Azevedo, and A. Falcão. A general image processing architecture for fpga. In *V Southern Programmable Logic Conference*, pages 27–32, São Carlos, SP, 2009. Rima.

[4] A.X. Falcão, B. S. da Cunha, and R. A. Lotufo. Design of connected operators using the image foresting transform. In *SPIE on Medical Imaging*, volume 4322, pages 468–479, Feb 2001.

[5] R. Audigier and R.A. Lotufo. Watershed by image foresting transform, tie-zone, and theoretical relationship with other watershed definitions. In *Mathematical Morphology and its Applications to Signal and Image Processing (ISMM)*, pages 277–288, Rio de Janeiro, RJ, Oct 2007. MCT/INPE.

[6] P.A.V. Miranda and A.X. Falcão. Links between image segmentation based on optimum-path forest and minimum cut in graph. *Journal of Mathematical Imaging and Vision*, 2009. to appear.

[7] R.A. Lotufo, A.X. Falcão, and F. Zampirolli. IFT-Watershed from gray-scale marker. In *XV Brazilian Symp. on Computer Graphics*

and Image Processing (SIBGRAPI), pages 146–152. IEEE, Oct 2002.

[8] A.X. Falcão, P.A.V. Miranda, and A. Rocha. A linear-time approach for image segmentation using graph-cut measures. In *8th Intl. Conf. on Advanced Concepts for Intelligent Vision Systems (ACIVS)*, volume LNCS 4179, pages 138–149, Antwerp, Belgium, 2006. Springer.

[9] F.P.G. Bergo, A.X. Falcão, P.A.V. Miranda, and L.M. Rocha. Automatic image segmentation by tree pruning. *Journal of Mathematical Imaging and Vision*, 29(2–3):141–162, Nov 2007.

[10] L.M. Rocha, F.A.M. Cappabianco, and A.X. Falcão. Data clustering as an optimum-path forest problem with applications in image analysis. *Intl. Journal of Imaging Systems and Technology*, 19(2):50–68, Jun 2009.

[11] J.P. Papa, A.X. Falcão, and C.T.N. Suzuki. Supervised pattern classification based on optimum-path forest. *Intl. Journal of Imaging Systems and Technology*, 19(2):120–131, Jun 2009.

[12] A. X. Falcão and F. P. G. Bergo. Interactive volume segmentation with differential image foresting transforms. *IEEE Trans. on Medical Imaging*, 23(9):1100–1108, 2004.

[13] F.P.G. Bergo and A.X. Falcão. A partitioned algorithm for the image foresting transform. In *Mathematical Morphology and its Applications to Signal and Image Processing (ISMM)*, pages 425–436, Rio de Janeiro, RJ, Oct 2007. MCT/INPE.

[14] I. Ragnemalm. Fast erosion and dilation by contour processing and thresholding of distance maps. *Pattern Recognition Letters*, 13:161–166, Mar 1992.

[15] A.X. Falcão, J.K. Udupa, and F.K. Miyazawa. An ultra-fast user-steered image segmentation paradigm: Live-wire-on-the-fly. *IEEE Trans. on Medical Imaging*, 19(1):55–62, Jan 2000.

[16] A.X. Falcão, L.F. Costa, and B.S. da Cunha. Multiscale skeletons by image foresting transform and its applications to neuromorphometry. *Pattern Recognition*, 35(7):1571–1582, Apr 2002.

[17] R.S. Torres, A.X. Falcão, and L.F. Costa. A graph-based approach for multiscale shape analysis. *Pattern Recognition*, 37(6):1163–1174, 2004.

[18] R.S. Torres and A.X. Falcão. Contour salience descriptors for effective image retrieval and analysis. *Image and Vision Computing*, 25(1):3–13, Jan 2007.

[19] F.A. Andaló, P.A.V. Miranda, R.S. Torres, and A.X. Falcão. Detecting contour saliences using tensor scale. In *14th IEEE Intl. Conf. on Image Processing*, volume VI, pages 349–352, San Antonio, Texas, Sep 2007.

[20] F.A. Andaló, P.A.V. Miranda, R.S. Torres, and A.X. Falcão. A new shape descriptor based on tensor scale. In *Mathematical Morphology and its Applications to Signal and Image Processing (ISMM)*, pages 141–152, Rio de Janeiro, RJ, Oct 2007. MCT/INPE.

[21] R.A. Lotufo and A.X. Falcão. The ordered queue and the optimality of the watershed approaches. In *Mathematical Morphology and its Applications to Image and Signal Processing (ISMM)*, volume 18, pages 341–350. Kluwer, Jun 2000.

[22] A.X. Falcão, J.K. Udupa, S. Samarasekera, S. Sharma, B.E. Hirsch, and R.A. Lotufo. User-steered image segmentation paradigms: Live wire and live lane. *Graphical Models and Image Processing*, 60(4):233–260, Jul 1998.

[23] A.X. Falcão and J.K. Udupa. A 3D generalization of user-steered live wire segmentation. *Medical Imaging Analysis*, 4(4):389–402, Dec 2000.

[24] A. X. Falcão, F. P. G. Bergo, and P. A. V. Miranda. Image segmentation by tree pruning. In *XVII Brazilian Symp. on Computer Graphics and Image Processing (SIBGRAPI)*, pages 65–71. IEEE, Oct 2004.

[25] L.G. Nyúl, A.X. Falcão, and J.K. Udupa. Fuzzy-connected 3D image segmentation at interactive speeds. *Graphical Models*, 64(5):259–281, 2003.

[26] P.A.V. Miranda, A.X. Falcão, A. Rocha, and F.P.G. Bergo. Object delineation by κ-connected components. *EURASIP Journal on Advances in Signal Processing*, 2008.

[27] J.P. Papa and A.X. Falcão. A new optimum-path forest approach for supervised classification. In *Proc. of the 4th Intl. Symp. on Visual Computing*, volume LNCS 5358, pages 935–944, Las Vegas, Nevada, 2008. Springer.

[28] J.P. Papa and A.X. Falcão. A learning algorithm for the optimum-path forest classifier. In *Proc. of the 7th IAPR TC-15 Workshop on Graph-based Representations in Pattern Recognition*, volume LNCS 5534, pages 195–204, Venice, Italy, 2009. Springer.

[29] T.V. Spina, J.A. Montoya-Zegarra, A.X. Falcão, and P.A.V. Miranda. Fast interactive segmentation of natural images using the image foresting transform. In *Proc. of the 16th Intl. Conf. on Digital Signal Processing*, Santorini, Greece, 2009. IEEE. to appear.

[30] J.A. Montoya-Zegarra, J.P. Papa, N.J. Leite, R.S. Torres, and A.X. Falcão. Learning how to extract rotation-invariant and scale-invariant features from texture images. *EURASIP Journal on Advances in Signal*, 2008.

[31] M.S. Scordilis, J.P. Papa A.I. Iliev, and A.X. Falcão. Spoken emotion recognition through optimum-path forest classification using glottal features. *Computer Speech and Language*, 2009.

[32] J.A. Montoya-Zegarra, J.P. Papa, N.J. Leite, R.S. Torres, and A.X. Falcão. Novel approaches for exclusive and continuous fingerprint classification. In *Proc. of the 3rd Pacific-Rim Symposium on Image and Video Technology (PSVIT 2009)*, volume LNCS 5414, pages 386–397, Tokyo, Japan, 2008. Springer.

[33] J.P. Papa, A.X. Falcão, A.M. Levada, D. Corrêa, D. Salvadeo, and N.D.A. Mascarenhas. Fast and accurate holistic face recognition using optimum-path forest. In *Proc. of the 16th Intl. Conf. on Digital Signal Processing*, Santorini, Greece, 2009. IEEE. to appear.

[34] G. Chiachia, A.N. Marana, J.P. Papa, and A.X. Falcão. Infrared face recogniton by optimum-path forest. In *Proc. of the 16th Intl.*

Conf. on Systems, Signals, and Image Processing, Chalkida, Greece, 2009. IEEE. to appear.

[35] R.J. Pisani, J.P. Papa, C.R.L. Zimback, A.X. Falcão, and A.P. Barbosa. Land use classification using optimum-path forest. In *XIV Brazilian Remote Sensing Symposium (SBSR)*, pages 7063–7070, Natal-RN, 2009. MCT-INPE.

[36] G.M. Freitas, A.M.H. Ávila, H.S. Pinto, J.P. Papa, and A.X. Falcão. Optimum-path forest-based models for rainfall estimation. In *Proc. of the 16th Intl. Conf. on Systems, Signals and Image Processing*, Chalkida, Greece, 2009. IEEE. to appear.

[37] R. Minetto, J.P. Papa, T.V. Spina, A.X. Falcão, N.J. Leite, and J. Stolfi. Fast and robust object tracking using image foresting transform. In *Proc. of the 16th Intl. Conf. on Systems, Signals, and Image Processing*, Chalkida, Greece, 2009. IEEE. to appear.

[38] P.A.V. Miranda, A.X. Falcão, and J.K. Udupa. *CLOUDS*: A model for synergistic image segmentation. In *The Fifth IEEE Intl. Symp. on Biomedical Imaging (ISBI)*, pages 209–212, Paris, France, 2008.

[39] P.A.V. Miranda, A.X. Falcão, and J.K. Udupa. Cloud bank: A multiple clouds model and its use in mr brain image segmentation. In *The Sixth IEEE Intl. Symp. on Biomedical Imaging: From Nano to Macro (ISBI)*, Boston, MA, 2009. to appear.

[40] F. Cappabianco, A.X. Falcão, and L.M. Rocha. Clustering by optimum path forest and its application to automatic GM/WM

classification in MR-T1 images of the brain. In *The Fifth IEEE Intl. Symp. on Biomedical Imaging (ISBI)*, pages 428–431, Paris, France, 2008.

[41] A.A. Spadotto, J.C. Pereira, R.C. Guido, J.P. Papa, A.X. Falcão, A.R. Gatto, P.C. Cola, and A.O. Schelp. Oropharyngeal dysphagia identification using wavelets and optimum path forest. In *3rd IEEE Intl. Symp. on Communications, Control and Signal Processing*, pages 735–740, St. Julians, Malta, 2008.

[42] J.P. Papa, A.A. Spadotto, A.X. Falcão, and J.C. Pereira. Optimum path forest classifier applied to laryngeal pathology detection. In *Proc. of the 15th Intl. Conf. on Systems, Signals, and Image Processing*, pages 249–252, Bratislava, Slovakia, 2008. IEEE.